*Inorg. Chem.* **2008**, *47*, 7921−7927

# Construction of Subphthalocyanine−Porphyrin and Subphthalocyanine−Phthalocyanine Heterodyads through Axial Coordination

**Hu Xu and Dennis K. P. Ng***

*Department of Chemistry and Center of Novel Functional Molecules, The Chinese University of Hong Kong, Shatin, N.T., Hong Kong, China*

Received April 30, 2008

The treatment of boron(III) subphthalocyanine chloride (SPcCl) with 3- or 4-hydroxypyridine in the presence of pyridine in toluene gave the corresponding boron(III) subphthalocyanine pyridinolates SPc(3-OPy) (**1**) or SPc(4-OPy) (**2**). Having a pyridyl group, these compounds could axially complex with a series of zinc(II) and ruthenium(II) porphyrins and phthalocyanines to form the corresponding subphthalocyanine−porphyrin and subphthalocyanine−phthalocyanine heterodyads. As revealed by UV−vis spectroscopy, the ground-state interaction between the two chromophores in these dyads is insignificant. The complexation processes were also studied by $^1$H NMR and fluorescence spectroscopic methods, which confirmed the 1:1 binding stoichiometry. The association constants, as determined by fluorescence titration, were generally higher for the ruthenium(II) tetrapyrroles [(2.5−4.7) × $10^4$ $M^{-1}$] than for the zinc(II) counterparts [(0.3−1.8) × $10^4$ $M^{-1}$]. The molecular structures of the two pyridyl subphthalocyanines **1** and **2**, together with three novel subphthalocyanine−porphyrin heterodyads, were also determined by X-ray diffraction analyses.

## Introduction

Porphyrins, phthalocyanines, and subphthalocyanines are structurally related cyclic oligopyrrole derivatives. The former two classes of macrocycles have long been known as versatile functional pigments,[1] while the last series have received considerable attention only for about a decade.[2] Having a different $\pi$-conjugated skeleton, these macrocycles show distinct optical and electronic properties, rendering them to find applications in different areas. Hybridization of these chromophores, which show complementary absorptions in the visible region, can extend the absorption region and generate new species and properties through interchromophoric interactions. Photoinduced energy and electron transfers are two common and important processes that can lead to useful applications in light harvesting, photovoltaics, and molecular photonics.[3] A substantial number of covalent and noncovalent porphyrin−phthalocyanine heteroarrays have been reported.[4] By contrast, subphthalocyanines conjugated with tetrapyrrole derivatives are extremely rare. To our knowledge, only two covalent subphthalocyanine−phthalocyanine dyads have been reported so far.[5] We[6] and Cook et al.[7] have recently employed the axial coordination approach to construct a series of mixed porphyrin−phthalocyanine heterodyads to pentads. We report herein an extension of this work using subphthalocyanines with an axial pyridyl group to complex with a series of zinc(II) and ruthenium(II)

* To whom correspondence should be addressed. E-mail: dkpn@cuhk.edu.hk.

(1) *The Porphyrin Handbook*; Kadish, K. M., Smith, K. M., Guilard, R., Eds.; Academic Press: San Diego, 2000; Vols. 1−10, 2003; Vols. 11−20.

(2) (a) Geyer, M.; Plenzig, F.; Rauschnabel, J.; Hanack, M.; del Rey, B.; Sastre, A.; Torres, T. *Synthesis* **1996**, 1139. (b) Claessens, C. G.; González-Rodríguez, D.; Torres, T. *Chem. Rev.* **2002**, *102*, 835.

(3) (a) Holten, D.; Bocian, J. S.; Lindsey, J. S. *Acc. Chem. Res.* **2002**, *35*, 57. (b) Kobuke, Y.; Ogawa, K. *Bull. Chem. Soc. Jpn.* **2003**, *76*, 689. (c) Wasielewski, M. R. *J. Org. Chem.* **2006**, *71*, 5051. (d) Balzani, V.; Credi, A.; Venturi, M. *Chem.—Eur. J.* **2008**, *14*, 26.

(4) Lo, P.-C.; Leng, X.; Ng, D. K. P. *Coord. Chem. Rev.* **2007**, *251*, 2334.

(5) (a) González-Rodríguez, D.; Claessens, C. G.; Torres, T.; Liu, S.; Echegoyen, L.; Vila, N.; Nonell, S. *Chem.—Eur. J.* **2005**, *11*, 3881. (b) Tolbin, A. Yu.; Breusova, M. O.; Pushkarev, V. E.; Tomilova, L. G. *Russ. Chem. Bull., Int. Ed.* **2005**, *54*, 2083.

(6) (a) Li, X.-Y.; Ng, D. K. P. *Eur. J. Inorg. Chem.* **2000**, 1845. (b) Choi, M. T. M.; Choi, C.-F.; Ng, D. K. P. *Tetrahedron* **2004**, *60*, 6889. (c) Leng, X.; Ng, D. K. P. *Eur. J. Inorg. Chem.* **2007**, 4615.

(7) (a) Berber, G.; Cammidge, A. N.; Chambrier, I.; Cook, M. J.; Hough, P. W. *Tetrahedron Lett.* **2003**, *44*, 5527. (b) Cammidge, A. N.; Berber, G.; Chambrier, I.; Hough, P. W.; Cook, M. J. *Tetrahedron* **2005**, *61*, 4067.

10.1021/ic800756h CCC: $40.75 
Published on Web 07/29/2008

**Chart 1**

Pyridyl Subphthalocyanines

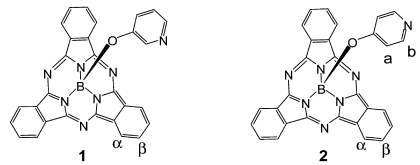

**1** **2**

Metallo Porphyrins and Phthalocyanines

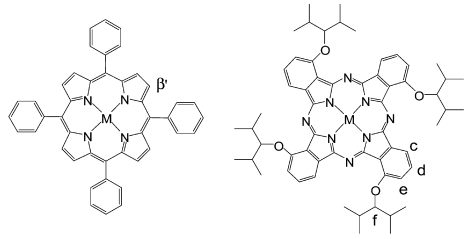

**3** M = Zn
**4** M = Ru(CO)

**5** M = Zn
**6** M = Ru(CO)

porphyrins and phthalocyanines to form the corresponding heterodyads. It is worth noting that the self-assembly of subphthalocyanines remains little studied. Torres et al. have recently synthesized two novel subphthalocyanines substituted with three peripheral pyridyl groups, which, in the presence of palladium(II) ions, self-assemble to form $M_3L_2$-type subphthalocyanine cages.[8] The present work uses the axial ligand instead of the peripheral groups of subphthalocyanines for complexation and can therefore extend the supramolecular chemistry of this interesting class of macrocycles.

## Results and Discussion

Subphthalocyanines SPc(3-OPy) (**1**) and SPc(4-OPy) (**2**) (Chart 1) containing an axial pyridyl group were prepared by ligand substitution reactions of the commercially available boron(III) subphthalocyanine chloride (SPcCl) with 3- or 4-hydroxypyridine in moderate yields. Both compounds were fully characterized spectroscopically and structurally. Single crystals of these compounds were grown by layering hexane onto their concentrated chloroform solutions. Compound **1** crystallizes in the triclinic system. As shown in Figure 1a, the boron center is tetracoordinated with three isoindole nitrogen atoms in a cone-shaped macrocycle and a pyridyloxy group. The B−O bond distance [1.463(5) Å] and the average B−N bond distance [1.502(6) Å] as well as the other structural data are comparable with those found in the 1,1′-binaphthyl-2,2′-dioxy-bridged bis(subphthalocyanine) [1.428(3) and 1.436(2) Å (for B−O bonds); 1.500(3) and 1.490(3) Å (for B−N bonds)].[9] Compound **2** (Figure 1b) crystallizes in the monoclinic system. The B−O [1.440(2) Å] and average B−N [1.494(2) Å] bond distances are close to those in **1**. The B−O−C bond angles of these two compounds [116.2(3)° and 118.63(12)° for **1** and **2**, respectively] are also similar.

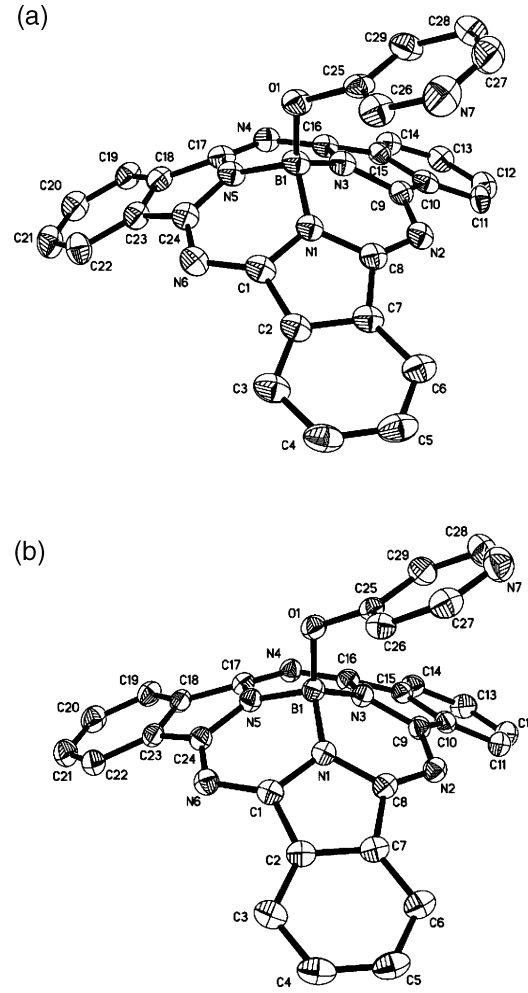


**Figure 1.** Molecular structures of (a) **1** and (b) **2** showing the 30% probability thermal ellipsoids for all non-hydrogen atoms.

For the tetrapyrrole components, both zinc(II) and ruthenium(II) ions were selected as the metal centers because of their well-known binding behavior with pyridyl ligands.[10] The structures of the four compounds involved in this study (**3**−**6**) are also shown in Chart 1. The ruthenium(II) porphyrin Ru(CO)TPP (TPP = *meso*-tetraphenylporphyrinate; **4**)[11] and the zinc(II) phthalocyanine $ZnPc(OC_7H_{15})_4$ [$Pc(OC_7H_{15})_4$ = 1,8,15,22-tetrakis(1-isopropyl-2-methylpropoxy)phthalocyaninate; **5**][12] were prepared by the literature method, while the ruthenium(II) analogue $Ru(CO)Pc(OC_7H_{15})_4$ (**6**) was prepared by treatment of the corresponding metal-free phthalocyanine $H_2Pc(OC_7H_{15})_4$[13] with $Ru_3(CO)_{12}$ in refluxing benzonitrile.

The complexation of **1** and ZnTPP (**3**) was first studied and monitored using $^1$H NMR spectroscopy. Figure 2 shows the $^1$H NMR spectra of their mixtures in different mole fractions. It can be seen that the signals for all of the subphthalocyanine [$H_\alpha$ at $\delta$ 8.84−8.88 and $H_\beta$ at $\delta$ 7.91−7.95]

(8) (a) Claessens, C. G.; Torres, T. *J. Am. Chem. Soc.* **2002**, *124*, 14522. (b) Claessens, C. G.; Torres, T. *Chem. Commun.* **2004**, 1298.
(9) Fukuda, T.; Olmstead, M. M.; Durfee, W. S.; Kobayashi, N. *Chem. Commun.* **2003**, 1256.
(10) Iengo, E.; Zangrando, E.; Alessio, E. *Eur. J. Inorg. Chem.* **2003**, 2371.
(11) Rillema, D. P.; Nagle, J. K.; Barringer, L. F., Jr.; Meyer, T. J. *J. Am. Chem. Soc.* **1981**, *103*, 56.
(12) Liu, W.; Lee, C.-H.; Chan, H.-S.; Mak, T. C. W.; Ng, D. K. P. *Eur. J. Inorg. Chem.* **2004**, 286.
(13) (a) Liu, W.; Lee, C.-H.; Li, H.-W.; Lam, C.-K.; Wang, J.; Mak, T. C. W.; Ng, D. K. P. *Chem. Commun.* **2002**, 628. (b) Lee, C.-H.; Ng, D. K. P. *Tetrahedron Lett.* **2002**, *43*, 4211.

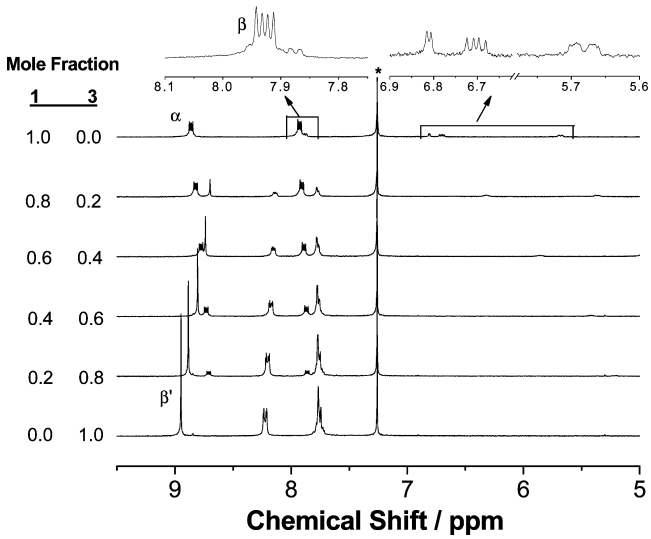


**Figure 2.** $^1$H NMR spectra of mixtures of **1** and **3** in different mole fractions in $CDCl_3$. The total concentration of **1** and **3** was fixed at 2.0 mM. The asterisk denotes residual $CHCl_3$. α and $\beta$ indicate the signals for the subphthalocyanine α and $\beta$ ring protons of **1**, while $\beta'$ indicates the signal for the $\beta$-pyrrole protons of **3**.

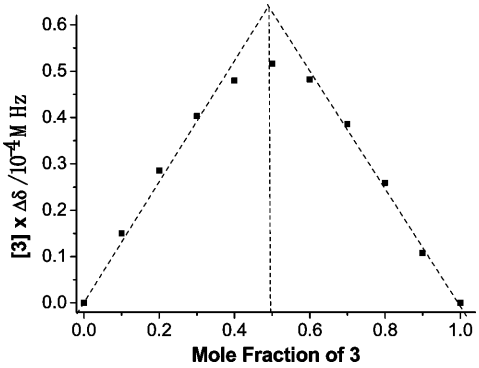


**Figure 3.** Modified Job's plot for the complexation of **1** and **3** in $CDCl_3$ by monitoring of the shift of the $^1$H NMR signal of the $\beta'$ protons of **3**.

and porphyrin [$H_{\beta'}$ at $\delta$ 8.95] ring protons are shifted upfield upon the addition of their coordinated partners. The signals for the pyridyl protons of **1** [at $\delta$ 7.88 (d), 6.81 (d), 6.71 (dd), and 5.68 (virtual d)] become weaker and eventually vanish as the mole fraction of **3** increases. Replacement of **3** with the metal-free analogue $H_2$TPP did not cause any shift of the $^1$H NMR signals. All of these observations clearly indicate the existence of axial coordination of the zinc(II) center of **3** with the pyridyl group of **1**. The upfield shift of the ring protons' signals is due to the ring current generated by the coordinated partner, while the broadening of the pyridyl protons' signals suggests that the binding is rather weak and there is extensive exchange between the coordinated and free pyridyl groups. Figure 3 shows the corresponding Job's plot[14] by monitoring of the shift of the singlet for $H_{\beta'}$. The maximum appears when the mole fraction of **3** is about 0.5, which confirms the 1:1 binding stoichiometry and the formation of the heterodyad SPc(3-OPy)−ZnTPP (**1**·**3**).

The complexation of the 4-pyridyl subphthalocyanine **2** and the ruthenium(II) phthalocyanine **6** was also studied in a similar manner. Figure 4 shows part of the $^1$H NMR spectra of their mixtures in different mole fractions in $CDCl_3/CD_3OD$ (40:1, v/v). The spectral changes are different from those observed for **1**·**3** described above. As the mole fraction of the coordinated partner increases, all of the signals for both **2** and **6** are weakened and broadened but do not shift significantly. Concomitantly, a new set of signals appears that can be attributed to the 1:1 heterodyad SPc(4-OPy)−Ru(CO)Pc($OC_7H_{15}$)$_4$ (**2**·**6**). This observation suggests that the exchange between the complexed and the free macrocycles is slow on the NMR time scale, which may be attributed to the generally stronger binding between pyridyl ligands and ruthenium(II) macrocycles compared with the zinc(II) counterparts.[15] Interestingly, at 1:1 ratio (mole fraction = 0.5 for both components), all of the signals for the uncomplexed **2** and **6** essentially vanish, leaving only the signals for the dyad **2**·**6**. As indicated in the figure, all of the signals of **2** and **6** are shifted upfield upon complexation as a result of the shielding by the coordinated partner. The doublet at $\delta$ 3.2 is tentatively assigned to the pyridyl protons $H_a$ of **2**·**6**. However, the signal for the pyridyl protons $H_b$, which should be more upfield-shifted by the ring current of **6**, cannot be observed and is probably masked by the signals of the 2,4-dimethyl-3-pentoxy substituent. To reveal the location of this signal, the $^1$H−$^1$H COSY spectrum of an equimolar mixture of **2** and **6** in $CDCl_3/CD_3OD$ (40:1, v/v) was also recorded (Figure S1 in the Supporting Information). A cross peak was clearly seen for the doublet at $\delta$ 3.2 and the doublet at $\delta$ 1.5, which is due to one of the methyl groups. Hence, the signal of the pyridyl protons $H_b$ is embedded in this methyl doublet. The signal is greatly shifted upfield (from $\delta$ 7.8 to 1.5) upon coordination to **6**.

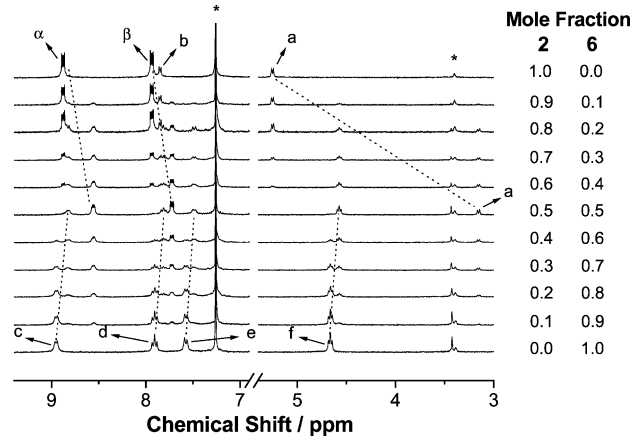


**Figure 4.** Part of the $^1$H NMR spectra of mixtures of **2** and **6** in different mole fractions in $CDCl_3/CD_3OD$ (40:1, v/v). The total concentration of **2** and **6** was fixed at 2.0 mM. The asterisk denotes residual solvent signals. For the other notations for proton assignments, refer to Chart 1.

The formation of all of the heterodyads between subphthalocyanines **1** and **2** and phthalocyanines **5** and **6** was also confirmed by electrospray ionization (ESI) mass spectrometry. For all of the four dyads, the protonated molecular ion ($MH^+$) envelope of which the isotopic distribution was in

(14) Hirose, K. *J. Inclusion Phenom. Macrocyclic Chem.* **2001**, *39*, 193.

(15) (a) Kleij, A. W.; Kuil, M.; Tooke, D. M.; Spek, A. L.; Reek, J. N. H. *Inorg. Chem.* **2005**, *44*, 7696. (b) Gunter, M. J.; Mullen, K. M. *Inorg. Chem.* **2007**, *46*, 4876.

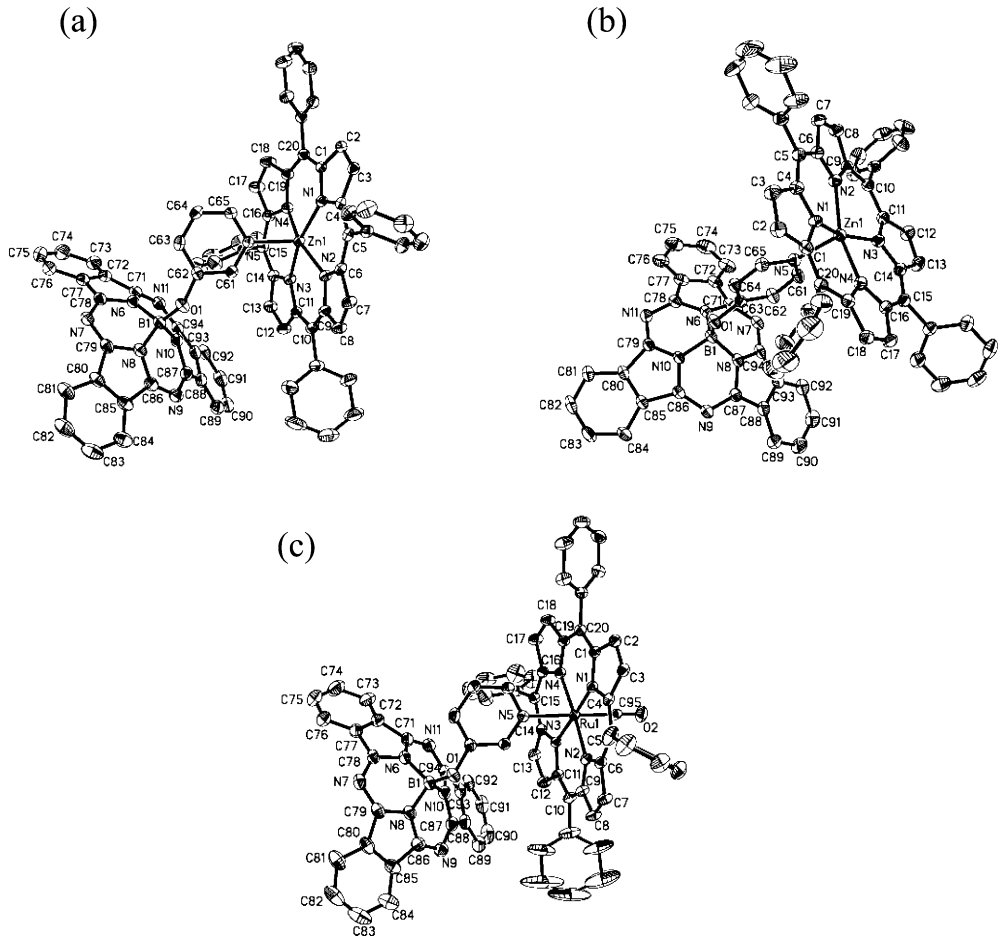


**Figure 5.** Molecular structures of (a) **1·3**, (b) **2·3**, and (c) **1·4** showing the 30% probability thermal ellipsoids for all non-hydrogen atoms.

good agreement with the simulated pattern (Figures S2 and S3 in the Supporting Information) was detected. Accurate mass measurements also gave very satisfactory results.[16]

The solid-state IR spectra of the ruthenium(II) tetrapyrroles **4** and **6** showed strong CO stretching bands at 1947 and 1961 $cm^{-1}$, respectively. For their complexes with the pyridyl subphthalocyanines **1** and **2** isolated from their corresponding mixtures in chloroform, the CO stretching frequency increased by 6−10 $cm^{-1}$. Similar changes have also been observed for related systems reported previously.[7b,17]

An unambiguous proof of the formation of these heterodyads came from the X-ray diffraction studies. Purple single crystals of SPc(3-OPy)−ZnTPP (**1·3**), SPc(4-OPy)−ZnTPP (**2·3**), and SPc(3-OPy)−Ru(CO)TPP (**1·4**) with different solvents of crystallization were obtained by slow evaporation of their saturated chloroform solutions containing a small amount of acetone and tetrahydrofuran (THF). All of the dyads crystallize in the triclinic system with a space group of $P\bar{1}$. Figure 5 shows the molecular structures of these dyads. For the dyads involving ZnTPP [**1·3** (Figure 5a) and **2·3** (Figure 5b), the Zn−N(pyridyl) bond distances [2.155(3) and 2.1509(9) Å, respectively] are slightly longer than the corresponding averages of the Zn−N(TPP) distance [2.066(2) and 2.0679(11) Å, respectively]. The data are close to those found in the heterodyad of ZnTPP and a pyridyl fullerene [Zn−N(pyridyl) = 2.158(5) Å; average Zn−N(TPP) = 2.075(5) Å].[18] Compared with the Zn−N(pyridyl) bond distance (2.4736 Å) of a diaxially pyridyl-coordinated ZnTPP,[15a] in which the zinc(II) center is hexacoordinated, the Zn−N(pyridyl) distances in **1·3** and **2·3** are much smaller. The zinc center in these dyads adopts a typical square-pyramidal geometry with a displacement of 0.293 Å (for **1·3**) or 0.359 Å (for **2·3**) above the porphyrin $N_4$ plane. The displacement is significantly larger for the latter. It is worth noting that the B−O−C bond angle is significantly increased upon complexation, from 116.2(3)° for **1** to 124.9(3)° for **1·3** and from 118.63(12)° for **2** to 129.85(10)° for **2·3**, probably for better complexation and reduction of the steric hindrance between the two large macrocycles.

As shown in Figure 5c, the ruthenium center of **1·4** adopts an octahedral geometry with the carbonyl and 3-pyridyl groups at the trans positions. The Ru−N(pyridine) [2.204(2)

(16) For **1·5**, HRMS (ESI). Calcd for $C_{89}H_{89}BN_{15}O_5Zn$ ($MH^+$): 1522.6550. Found: 1522.6547. For **2·5**, HRMS (ESI). Calcd for $C_{89}H_{89}BN_{15}O_5Zn$ ($MH^+$): 1522.6550. Found: 1522.6562. For **1·6**, HRMS (ESI). Calcd for $C_{90}H_{89}BN_{15}O_6Ru$ ($MH^+$): 1588.6251. Found: 1588.6253. For **2·6**, HRMS (ESI). Calcd for $C_{90}H_{89}BN_{15}O_6Ru$ ($MH^+$): 1588.6251. Found: 1588.6262.

(17) (a) Webb, S. J.; Sanders, J. K. M. *Inorg. Chem.* **2000**, *39*, 5912. (b) Stulz, E.; Maue, M.; Feeder, N.; Teat, S. J.; Ng, Y.-F.; Bond, A. D.; Darling, S. L.; Sanders, J. K. M. *Inorg. Chem.* **2002**, *41*, 5255. (c) Stulz, E.; Maue, M.; Scott, S. M.; Mann, B. E.; Sanders, J. K. M. *New J. Chem.* **2004**, *28*, 1066.

(18) D'Souza, F.; Rath, N. P.; Deviprasad, G. R.; Zandler, M. E. *Chem. Commun.* **2001**, 267.

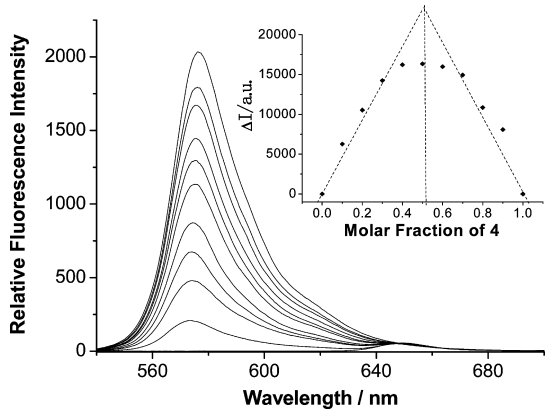


**Figure 6.** Fluorescence spectra of mixtures of **2** and **4** in DMF (excited at 510 nm). The total concentration of the two compounds was fixed at 10.0 $\mu$M. The inset shows the corresponding Job's plot by monitoring of the area of the fluorescence peak.

Å], average Ru−N(TPP) [2.050(2) Å], and Ru−C(CO) [1.828(3) Å] bond distances compare well with those found in Ru(CO)(Py)TPP (Py = pyridine) [2.193(4), 2.052(9), and 1.838(9) Å, respectively][19] and the porphyrin dyad $H_2$-(3′MPyP)·Ru(CO)TPP [$H_2$(3′MPyP) = 5-(3′-pyridyl)-10,15,20-triphenylporphyrin] [2.189(2), 2.054(2), and 1.844(3) Å, respectively].[20] The B−O−C angle of this dyad [125.0(2)°] is also larger than that of **1** [116.2(3)°].

Upon the addition of the pyridyl subphthalocyanine **1** or **2** (up to 4 equiv with respect to **3**−**6**), the Soret band of porphyrins **3** and **4** and the Q band of phthalocyanines **5** and **6** were not changed in *N*,*N*-dimethylformamide (DMF). In chloroform, the shifts were at most 2 nm for **3**, **4**, and **6**, while that for **5** was again negligible. These observations suggested that the ground-state interactions between the two chromophores in these dyads are not significant, particularly in coordinating solvents.

The complexation of the pyridyl subphthalocyanines **1** and **2** and the tetrapyrroles **3**−**6** was also studied by fluorescence spectroscopy. Figure 6 shows the fluorescence spectra of mixtures of **2** and **4** in different mole fractions in DMF, where the total concentration was fixed at 10.0 $\mu$M. Upon excitation at 510 nm, the mixtures gave an emission band at 573−576 nm attributable to the subphthalocyanine **2**. When the area of the fluorescence peak was plotted versus the mole fraction of **4**, the curve showed a maximum at about 0.5 (inset of Figure 6). This again supported the formation of a 1:1 heterodyad between **2** and **4**.

Figure 7 shows the change in the fluorescence spectrum of **2** (5.0 $\mu$M) upon titration with **4** (from 0 to 21.5 $\mu$M). The fluorescence emission due to subphthalocyanine **2** at ca. 570 nm diminishes gradually, while a weak emission band at ca. 650 nm emerges, which is due to the porphyrin **4** added. The quenching of the emission of **2** by **4** is likely due to a photoinduced electron transfer. No emission due to **4** was observed when **2** was excited at 470 nm, which precluded an energy-transfer pathway. The association constant $K$ for the dyad **2**·**4** was determined by the

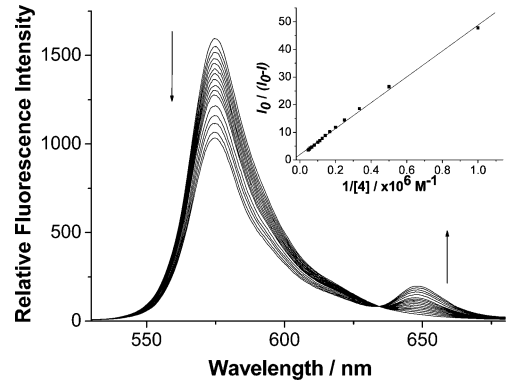


**Figure 7.** Change in the fluorescence spectrum of **2** (5.0 $\mu$M) upon titration with **4** (from 0 to 21.5 $\mu$M) in DMF (excited at 510 nm). The inset shows the corresponding Benesi−Hildebrand plot for the determination of their association constants.

Benesi−Hildebrand equation $I_0/(I_0 - I) = 1/A + 1/AK[\mathbf{4}]$, where $I_0$ and $I$ represent the fluorescence intensity of **2** without and with the addition of **4**, respectively, and $A$ is a constant related to the difference in the emission quantum yield of the complexed and uncomplexed **2**.[21] When $I_0/(I_0 - I)$ vs 1/[**4**] (inset of Figure 7) was plotted, a straight line was obtained from which the value of $K$ was determined to be $(4.2 \pm 0.5) \times 10^4$ M$^{-1}$.

The complexation of all of the other systems was also studied with the same approach. The binding stoichiometry was confirmed to be 1:1 in all cases. The corresponding association constants are summarized in Table 1. The values for ZnTPP fall into the range reported for the complexation of ZnTPP with pyridine (610−25 100 M$^{-1}$); the values appear to be significantly affected by the solvent.[22] They are also comparable with the values reported for the binding between pyridine and other zinc(II) *meso*-tetraarylporphyrins[23] and between pyridyl fullerenes and ZnTPP.[24] As shown in Table 1, the association constants for ZnTPP are about 3 times higher than those for **5**. The values for **5** are close to that reported for a $C_{60}$-appended pyridine and zinc(II) tetra-*tert*-butylphthalocyanine ($4.8 \times 10^3$ M$^{-1}$).[25] Generally, the binding of **1** and **2** with the ruthenium(II) tetrapyrroles **4** and **6** [$K = (2.5-4.7) \times 10^4$ M$^{-1}$] is stronger than the binding with the zinc(II) counterparts **3** and **5** [$K = (0.3-1.8) \times 10^4$ M$^{-1}$]. Apparently, the values for the ruthenium(II) tetrapyrroles are somewhat lower than expected, which may be due to the fact that the measurements were made in a coordinating solvent (DMF). It is noted that the association constants for a ruthenium(II) porphyrin and pyridine were also determined to be only 3000−9500 M$^{-1}$ in THF-$d_8$.[17a] In $CH_2Cl_2$, the value for **4** and pyridine was found to be

(19) Little, R. G.; Ibers, J. A. *J. Am. Chem. Soc.* **1973**, *95*, 8583.
(20) Alessio, E.; Geremia, S.; Mestroni, S.; Iengo, E.; Srnova, I.; Slouf, M. *Inorg. Chem.* **1999**, *38*, 869.
(21) Benesi, H. A.; Hildebrand, J. H. *J. Am. Chem. Soc.* **1949**, *71*, 2703.
(22) Ercolani, G.; Ioele, M.; Monti, D. *New J. Chem.* **2001**, *25*, 783.
(23) Ikeda, C.; Tanaka, Y.; Fujihara, T.; Ishii, Y.; Ushiyama, T.; Yamamoto, K.; Yoshioka, N.; Inoue, H. *Inorg. Chem.* **2001**, *40*, 3395.
(24) (a) Armaroli, N.; Diederich, F.; Echegoyen, L.; Habicher, T.; Flamigni, L.; Marconi, G.; Nierengarten, J.-F. *New J. Chem.* **1999**, 77. (b) D'Souza, F.; Deviprasad, G. R.; Zandler, M. E.; Hoang, Vu. T.; Klykov, A.; VanStipdonk, M.; Perera, A.; El-Khouly, M. E.; Fujitsuka, M.; Ito, O. *J. Phys. Chem. A* **2002**, *106*, 3243.
(25) Guldi, D. M.; Ramey, J.; Martínez-Díaz, M. V.; de la Escosura, A.; Torres, T.; Da Ros, T.; Prato, M. *Chem. Commun.* **2002**, 2774.

**Table 1.** Comparison of the Association Constants for Subphthalocyanines **1** and **2** and Tetrapyrroles **3**−**6**[a]

| | association constant ($K$)/$M^{-1}$ | | | |
|---|---|---|---|---|
| subphthalocyanine | ZnTPP (**3**) | Ru(CO)TPP (**4**) | $ZnPc(OC_7H_{15})_4$ (**5**) | $Ru(CO)Pc(OC_7H_{15})_4$ (**6**) |
| SPc(3-OPy) (**1**) | $(1.8 \pm 0.2) \times 10^4$ | $(4.2 \pm 0.4) \times 10^4$ | $(6.1 \pm 1.7) \times 10^3$ | $(2.5 \pm 0.4) \times 10^4$ |
| SPc(4-OPy) (**2**) | $(9.8 \pm 0.5) \times 10^3$ | $(4.2 \pm 0.5) \times 10^4$ | $(3.1 \pm 1.6) \times 10^3$ | $(4.7 \pm 0.4) \times 10^4$ |

[a] Determined by fluorescence titration in DMF.

**Table 2.** Crystallographic Data for Subphthalocyanines **1** and **2** and Their Axially Linked Dyads **1·3**, **1·4**, and **2·3**

| | **1** | **2** | **1·3**·1.5$C_3H_6O$ | **1·4** | **2·3**·$C_4H_8O$·$C_3H_6O$ |
|---|---|---|---|---|---|
| formula | $C_{29}H_{16}BN_7O$ | $C_{29}H_{16}BN_7O$ | $C_{77.5}H_{53}BN_{11}O_{2.5}Zn$ | $C_{74}H_{44}BN_{11}O_2Ru$ | $C_{80}H_{58}BN_{11}O_3Zn$ |
| $M_r$ | 489.30 | 489.30 | 1246.49 | 1231.08 | 1297.55 |
| cryst size ($mm^3$) | 0.50 × 0.40 × 0.30 | 0.40 × 0.30 × 0.20 | 0.50 × 0.40 × 0.30 | 0.50 × 0.40 × 0.30 | 0.50 × 0.40 × 0.30 |
| cryst syst | triclinic | monoclinic | triclinic | triclinic | triclinic |
| space group | $P\bar{1}$ | $P2_1/c$ | $P\bar{1}$ | $P\bar{1}$ | $P\bar{1}$ |
| $a$ (Å) | 10.173(11) | 12.440(2) | 14.2910(18) | 14.170(2) | 11.6308(16) |
| $b$ (Å) | 10.843(11) | 8.5676(16) | 14.3597(18) | 14.745(2) | 16.607(2) |
| $c$ (Å) | 11.845(12) | 21.371(4) | 19.097(2) | 19.094(3) | 17.987(3) |
| α (deg) | 85.80(2) | 90 | 70.607(2) | 68.285(3) | 101.665(3) |
| $\beta$ (deg) | 78.21(2) | 90.328(5) | 83.747(3) | 82.104(3) | 102.430(3) |
| $\gamma$ (deg) | 65.31(2) | 90 | 63.055(2) | 62.848(3) | 95.959(3) |
| $V$ ($Å^3$) | 1162(2) | 2277.8(7) | 3291.3(7) | 3295.6(8) | 3283.0(8) |
| $Z$ | 2 | 4 | 2 | 2 | 2 |
| $F$(000) | 504 | 1008 | 1292 | 1260 | 1348 |
| $\rho_{calcd}$ (mg $m^{-3}$) | 1.398 | 1.427 | 1.258 | 1.241 | 1.313 |
| $\mu$ ($mm^{-1}$) | 0.089 | 0.091 | 0.430 | 0.292 | 0.435 |
| $\theta$ range (deg) | 2.07−25.00 | 1.64−28.02 | 1.60−25.00 | 1.15−25.00 | 1.19−25.00 |
| no. of reflns collcd | 5378 | 15 025 | 17 782 | 17 860 | 17 902 |
| no. of indep reflns | 3760 ($R_{int}$ = 0.0328) | 5497 ($R_{int}$ = 0.0325) | 11 511 ($R_{int}$ = 0.0211) | 11 541 ($R_{int}$ = 0.0250) | 11 509 ($R_{int}$ = 0.0300) |
| no. of param | 344 | 343 | 856 | 802 | 910 |
| R1 [$I > 2\sigma(I)$] | 0.0786 | 0.0406 | 0.0499 | 0.0431 | 0.0469 |
| wR2 [$I > 2\sigma(I)$] | 0.2200 | 0.0924 | 0.1403 | 0.1151 | 0.1146 |
| GOF | 1.054 | 1.004 | 1.076 | 1.081 | 1.037 |

substantially higher ($4.3 \times 10^4$ $M^{-1}$)[26] and is just about 6-fold higher than that for ZnTPP ($K = 6.9 \times 10^3$ $M^{-1}$).[27]

## Conclusion

In summary, we have prepared two pyridyl subphthalocyanines **1** and **2**, which can complex with metalloporphyrins and -phthalocyanines **3**−**6** through axial coordination. The complexation processes of these macrocycles have been investigated in detail using various spectroscopic methods and X-ray diffraction analyses. The attachment of a subphthalocyanine ring does not significantly affect the binding behavior and strength of pyridine toward these tetrapyrrole derivatives. This simple approach allows the construction of noncovalent subphthalocyanine−porphyrin and subphthalocyanine−phthalocyanine dyads for the first time.

## Experimental Section

Experimental details regarding the purification of solvents and instrumentation were described elsewhere.[6c] Ru(CO)TPP (**4**),[11] $ZnPc(OC_7H_{15})_4$ (**5**),[12] and $H_2Pc(OC_7H_{15})_4$[13] were prepared according to the previously described methods.

**SPc(3-OPy) (1).** A mixture of boron(III) subphthalocyanine chloride (ca. 90%, 100 mg, 0.21 mmol), 3-hydroxypyridine (159 mg, 1.67 mmol), and pyridine (0.5 mL) in toluene (10 mL) was heated at reflux for 24 h. After cooling, the volatiles were removed under reduced pressure. The residue was then loaded onto a silica gel column and eluted with $CHCl_3$/MeOH (100:1, v/v). The crude product obtained was further purified by size exclusion chromatography with Bio-Beads S-X1 beads using THF as the eluent followed by recrystallization with acetone and hexane to give a violet solid (55 mg, 54%). $^1$H NMR (300 MHz, $CDCl_3$): $\delta$ 8.84−8.88 (m, 6 H, SPc-$H_\alpha$), 7.91−7.95 (m, 6 H, SPc-$H_\beta$), 7.88 (d, $J$ = 4.8 Hz, 1 H, Py-H), 6.81 (d, $J$ = 2.7 Hz, 1 H, Py-H), 6.71 (dd, $J$ = 4.8 and 8.1 Hz, 1 H, Py-H), 5.68 (virtual d, $J$ = 7.5 Hz, 1 H, Py-H). $^{13}$C{$^1$H} NMR (75.4 MHz, $CDCl_3$): $\delta$ 151.2, 149.0, 142.7, 141.9, 130.9, 129.9, 125.7, 123.3, 122.2. UV−vis (DMF) [$\lambda_{max}$ nm (log $\epsilon$)]: 306 (4.66), 510 (4.43), 562 (4.98). HRMS (ESI). Calcd for $C_{29}H_{17}BN_7O$ ($MH^+$): 490.1582. Found: 490.1591. Anal. Calcd for $C_{29}H_{16}BN_7O$: C, 71.19; H, 3.30; N, 20.04. Found: C, 71.27; H, 3.22; N, 19.92.

**SPc(4-OPy) (2).** According to the above procedure using 4-hydroxypyridine instead of 3-hydroxypyridine as the starting material, **2** was prepared as a violet solid (25 mg, 24%). $^1$H NMR (300 MHz, $CDCl_3$): $\delta$ 8.87−8.90 (m, 6 H, SPc-$H_\alpha$), 7.91−7.96 (m, 8 H, SPc-$H_\beta$ and Py-H), 5.26 (d, $J$ = 5.4 Hz, 2 H, Py-H). $^{13}$C{$^1$H} NMR (75.4 MHz, $CDCl_3$): $\delta$ 159.7, 151.6, 150.6, 130.9, 130.1, 122.3, 113.8. UV−vis (DMF) [$\lambda_{max}$ nm (log $\epsilon$)]: 303 (4.61), 507 (4.36), 564 (4.91). HRMS (ESI). Calcd for $C_{29}H_{17}BN_7O$ ($MH^+$): 490.1582. Found: 490.1577. Anal. Calcd for $C_{29}H_{16}BN_7O$: C, 71.19; H, 3.30; N, 20.04. Found: C, 71.68; H, 3.29; N, 20.09.

**$Ru(CO)Pc(OC_7H_{15})_4$ (6).** A mixture of the metal-free phthalocyanine $H_2Pc(OC_7H_{15})_4$ (50 mg, 0.05 mmol) and $Ru_3(CO)_{12}$ (66 mg, 0.10 mmol) in benzonitrile (2 mL) was heated at 200 °C for 1 h. After a brief cooling, the volatiles were removed under reduced pressure, then the residue was loaded onto a silica gel column and eluted with $CHCl_3$. The crude product was further purified by recrystallization with $CHCl_3$ and MeOH to give a dark blue powder (30 mg, 53%). $^1$H NMR (300 MHz, $C_6D_6$): $\delta$ 9.49 (d, $J$ = 7.5 Hz, 4 H, *Pc*-$H_\alpha$), 7.91 (virtual t, $J$ = 7.8 Hz, 4 H, Pc-$H_\beta$), 7.38 (d, $J$ = 8.4 Hz, 4 H, Pc-$H_{\beta'}$), 4.48 (t, $J$ = 5.7 Hz, 4 H, OCH), 2.51−2.57 (m, 8 H, CH), 1.62 (d, $J$ = 6.6 Hz, 12 H, $CH_3$), 1.55 (d, $J$ = 6.6 Hz, 12 H, $CH_3$), 1.09−1.14 (two overlapping d, 24 H, $CH_3$);

(26) Kadish, K. M.; Leggett, D. J.; Chang, D. *Inorg. Chem.* **1982**, *21*, 3618.
(27) Nappa, M.; Valentine, J. S. *J. Am. Chem. Soc.* **1978**, *100*, 5075.

$^{13}C\{^1H\}$ NMR (75.4 MHz, $CDCl_3$): $\delta$ 182.0, 158.2, 144.5, 144.4, 142.7, 129.7, 126.2, 114.2, 113.3, 89.5, 31.4, 31.3, 20.4, 20.2, 18.8, 18.3; UV−vis (DMF) [$\lambda_{max}$ nm (log $\epsilon$)]: 354 (4.46), 610 (4.72), 648 (4.68), 677 (5.41); HRMS (ESI) calcd for $C_{61}H_{73}N_8O_5Ru$ ($MH^+$) 1099.4742, found: 1099.4737. Anal. Calcd for $C_{62.5}H_{76.5}Cl_{1.5}N_8O_6Ru$ (**6**·0.5$CHCl_3$·$CH_3OH$): C, 63.08; H, 6.48; N, 9.42. Found: C, 62.80; H, 6.35; N, 9.45.

**X-ray Crystallographic Analyses.** Crystal data and details of data collection and structure refinement are given in Table 2. Data were collected on a Bruker SMART CCD diffractometer with a Mo Kα sealed tube ($\lambda$ = 0.710 73 Å) at 293 K, using a $\omega$ scan mode with an increment of 0.3°. Preliminary unit cell parameters were obtained from 45 frames. Final unit cell parameters were obtained by global refinements of reflections obtained from integration of all of the frame data. The collected frames were integrated using the preliminary cell-orientation matrix. *SMART* software was used for collecting frames of data, indexing reflections, and determining lattice constants, *SAINT-PLUS* for integrating the intensity of reflections and scaling,[29] *SADABS* for absorption correction,[29] and *SHELXL* for space group and structure determination, refinements, graphics, and structure reporting.[30]

**Acknowledgment.** This work was supported by a grant from the Research Grants Council of the Hong Kong Special Administrative Region, China (Project 402607), and a strategic investments scheme administered by The Chinese University of Hong Kong.

**Supporting Information Available:** $^1H-^1H$ COSY spectrum of **2**·**6**, comparison of the observed and simulated isotopic distribution for the $MH^+$ ion of all of the subphthalocyanine−phthalocyanine heterodyads, $^1H$ and $^{13}C$ NMR spectra of **1**, **2**, and **6**, and X-ray crystallographic data for **1**, **2**, **1**·**3**·1.5$C_3H_6O$, **1**·**4**, and **2**·**3**·$C_4H_8O$·$C_3H_6O$ in standard CIF format. This material is available free of charge via the Internet at http://pubs.acs.org.

IC800756H

(28) *SMART and SAINT for Windows NT Software Reference Manuals*, version 5.0; Bruker Analytical X-ray Systems: Madison, WI, 1997.

(29) Sheldrick, G. M. *SADABS—A Software for Empirical Absorption Correction*; University of Göttingen: Göttingen, Germany, 1997.

(30) *SHELXL Reference Manual*, version 5.1; Bruker Analytical X-ray Systems: Madison, WI, 1997.